Multi-scaling of the dense plasma focus

2015 J. Phys.: Conf. Ser. 591 012022

(http://iopscience.iop.org/1742-6596/591/1/012022)

Multi-scaling of the dense plasma focus

S H Saw[1,2,4] and S Lee[1,2,3]
[1]INTI International University, 71800 Nilai, Negeri Sembilan, Malaysia
[2]Institute of Plasma Focus Studies, Melbourne, Australia
[3]University Malaya, Kuala Lumpur, Malaysia

E-mail: sorheoh.saw@newinti.edu.my

Abstract. The dense plasma focus is a copious source of multi-radiations with many potential new applications of special interest such as in advanced SXR lithography, materials synthesizing and testing, medical isotopes and imaging. This paper reviews the series of numerical experiments conducted using the Lee model code to obtain the scaling laws of the multi-radiations.

1. Introduction

Plasma focus machines of various energies are increasingly being studied as sources of neutrons, soft x-rays and ions. An exciting prospect is for scaling the plasma focus up to regimes relevant for fusion energy studies. However, even a simple machine such as the UNU/ICTP PFF 3 kJ machine consistently produces 10^8 neutrons in deuterium [1]. Plasma focus machines operated in neon have also been studied as intense sources of soft x-rays [2-4]. Whilst many recent experiments have concentrated efforts on low energy repetitive devices [2-4], other experiments have looked at larger plasma focus devices [5, 6] extending to MJ regime. Numerical experiments are also gaining interest [7, 8] with the Lee model code [9] demonstrating that it computes realistic focus pinch parameters and absolute values of neutron yield Y_n and soft x-ray yield Y_{sxr} which are consistent with those measured experimentally. A comparison was made for the case of the NX2 machine [4], showing good agreement between computed and measured Y_{sxr} [8-10]. This gives confidence that the Lee model code gives realistic results in the computation of Y_n and Y_{sxr}.

In recent years, we see increasing investigations on the ion beams and plasma streams emission from PF devices. The motivation for these studies is the potential applications for materials synthesis, signatures and damage studies of candidate wall materials of fusion reactors. Hence we have extended our model code to enable numerical experiments to be carried out on defining properties of beam ions in various gases.

In this review, we show the comprehensive range of numerical experiments conducted to derive scaling laws on neutron yield Y_n [11, 12] and neon Y_{sxr} [8, 10], in terms of storage energy E_0, peak discharge current I_{peak} and peak focus pinch current I_{pinch} obtained from studies [13-15] carried out over E_0 varying from 0.2 kJ to 25 MJ for optimised machine parameters and operating parameters. We also present as yet unpublished results of the scaling of some beam ion defining properties.

2. The Lee Model Code

The Lee model code couples the electrical circuit with plasma focus dynamics, thermodynamics and radiation, enabling realistic simulation of all gross focus properties. The basic model, described in 1984 [16] was successfully used to assist several projects [17-19]. Radiation-coupled dynamics was included in the five-phase code leading to numerical experiments on radiation cooling [20]. The vital role of a finite small disturbance speed discussed by Potter in a Z-pinch situation [21] was incorporated together with real gas thermodynamics and radiation-yield terms. Before this 'communication delay effect' was incorporated, the model consistently over-estimated the radial speeds. This is serious from the point of view of neutron yields. A factor of two in shock speeds gives a factor of four in temperatures leading to a difference in fusion cross-sections of ~1000 at the range

of temperatures we are dealing with. This version of the code assisted other research projects [22-27] and was web-published in 2000 [28] and 2005 [29]. Plasma self-absorption was included in 2007 [27] improving SXR yield simulation. The code has been used extensively in several machines including UNU/ICTP PFF [1, 17, 22, 23, 25-27, 30, 31], NX2 [24, 27, 32], NX1 [3, 32] and adapted for the Filippov-type plasma focus DENA [33]. Neutron yield Y_n using a beam–target mechanism [11, 12, 14, 15, 34], is incorporated the code [9] (versions later than RADPFV5.13), resulting in realistic Y_n scaling with I_{pinch}[11, 12]. The versatility and utility of the model are demonstrated in its clear distinction of I_{pinch} from I_{peak}[13] and insights of current and neutron yield limitations [14, 15], neutron saturation [12, 35], radiative collapse[36] and current-stepped PF[37-39] and extraction of diagnostic data [13,40-45] and anomalous resistance data [46,47] from current signals. The description theory, code and a broad range of results of this 'Universal Plasma Focus Laboratory Facility' are available for download from [9]. We summarise the five phases used in the model code.

i) Axial Phase: Described by a snowplow model with an equation of motion coupled to a circuit equation. The equation of motion incorporates the axial phase model parameters: mass and current factors f_m and f_c [9,45,48-50] respectively; f_m accounting for the porosity of the current sheet, the inclination of the moving current sheet-shock front structure and all other unspecified effects which have effects equivalent to increasing or reducing mass in the moving structure; f_c accounting for the fraction of current effectively flowing in the moving structure (due to all effects including current shedding at or near the back-wall and current sheet inclination).

ii) Radial Inward Shock Phase: Described by four coupled equations using an elongating slug model. The first equation computes the radial inward shock speed from the driving magnetic pressure; the second the axial elongation speed of the column; the third the speed of the current sheath (aka the magnetic piston), allowing the current sheath to separate from the shock front by an adiabatic approximation. The fourth is the circuit equation. Thermodynamic effects due to ionization and excitation are incorporated, being important for gases other than hydrogen and deuterium. A communication delay between shock front and current sheath due to the finite small disturbance speed is crucially implemented. The model parameters, radial phase mass swept-up and current factors f_{mr} and f_{cr} respectively are incorporated in all three radial phases.

iii) Radial Reflected Shock (RS) Phase: When the shock front hits the axis, because the focus plasma is collisional, a RS develops which moves radially outwards, whilst the radial current sheath piston continues to move inwards. Four coupled equations are used, these being for the RS moving radially outwards, the piston moving radially inwards, the elongation of the annular column and the circuit. The plasma temperature behind the RS undergoes a jump by a factor of approximately two.

iv) Slow Compression (Quiescent) or Pinch Phase: When the out-going RS hits the in-coming piston the compression enters a radiative phase, with inclusion of energy loss/gain terms from Joule heating and radiation losses into the piston equation of motion; so that for gases such as krypton, radiation emission may enhance the compression. Three coupled equations describe this phase; the piston radial motion, the pinch column elongation and the circuit equations.

v) Expanded Column Phase: To simulate the current trace beyond this point, we allow the column to suddenly attain the radius of the anode. Two coupled equations are used; similar to the axial phase above.

2.1 Computation of Neutron Yield

The neutron yield is computed using a phenomenological beam-target neutron generating mechanism described recently by Gribkov et al [34]. A beam of fast deuteron ions is produced by diode action in a thin layer close to the anode, with plasma disruptions generating the necessary high voltages. The

beam interacts with the hot dense plasma of the focus pinch column to produce the fusion neutrons. The beam-target yield is derived [11, 12, 14, 28] as:

$$Y_{b\text{-}t} = C_n n_i I_{pinch}^2 z_p^2 (\ln(b/r_p))\, \sigma / U^{0.5} \quad (1)$$

where n_i = ion density, b = cathode radius, r_p = radius of the plasma pinch with length z_p, σ =cross-section of the D-D fusion reaction, n-branch [51] and U= beam energy. C_n is treated as a calibration constant combining various constants in the derivation process.

The D-D cross-section is sensitive to the beam energy in the range 15-150 kV. The code computes induced voltages (due to current motion inductive effects) V_{max} of the order of only 15-50 kV. However it is known, from experiments that the ion energy responsible for the beam-target neutrons is in the range 50-150 keV [34], and for smaller lower-voltage machines the relevant energy could be lower at 30-60 keV [31]. Fitting with extensive experimental observations of machines from sub-kJ to near MJ, the D-D cross section σ is reasonably obtained by using $U=3V_{max}$. A value of $C_n=2.7\text{x}10^7$ was obtained by calibrating the yield [9], [13]-[14] at an experimental point of 0.5 MA.

The thermonuclear component is also computed in every case and it is found that this component is negligible when compared with the beam-target component.

2.2 *Computation of Neon SXR Yield*

In the code [9, 32, 52], neon line radiation Q_L is calculated as follows:

$$dQ_L/dt = -4.6 \times 10^{-31} n_i^2 Z Z_n^4 (\pi r_p^2) z_f / T \quad (2)$$

where for the temperatures of interest in our experiments we take the SXR yield $Y_{sxr} = Q_L$. Z_n is the atomic number.

This generated energy is then reduced by the plasma self-absorption which is included by computing volumetric plasma self-absorption factor A derived from the photonic excitation number M which is a function of Z_n, n_i, Z and T. For SXR scaling there is an optimum small range of temperatures (around 200-500 eV T-window necessary to produce the He-like, H-like neon ions) [23, 24] to operate.

2.3 *Computation of Beam ion properties*

In the latest (2013 version) the Lee code computes the flux of the ion beams $J_b=n_b v_b$ where n_b=number of beam ions N_b divided by volume of plasma traversed is derived from pinch inductive energy considerations; and v_b=effective speed of the beam ions is derived from the accelerating voltage taken as diode voltage U. All quantities are expressed in SI units, except where otherwise stated. The resulting equation is given below:

$$\text{Flux} = J_b = 2.75\text{x}10^{15}\ (f_e/[MZ_{eff}]^{1/2})\{(\ln[b/r_p])/(r_p^2)\}(I_{pinch}^2)/U^{1/2} \quad \text{ions m}^{-2}\text{s}^{-1} \quad (3)$$

where M=ion mass, Z_{eff}=average effective charge of the ion in the pinch, b=cathode radius, r_p=pinch radius and I_{pinch}=pinch current. The parameter f_e = fraction of energy converted into beam energy from the inductive energy of the pinch. Analyzing neutron yield data [11, 14, 53, 54] and pinch dimensional-temporal relationships [22] we estimate f_e=0.14 and use the approximate scaling [22]: $\tau=10^{-6} z_p$. This condition f_e=0.14 is equivalent to ion beam energy of 3%-6% E_0 in the case when the pinch inductive energy holds 20%-40% of E_0. Our extensive study of high performance low inductance PF classified [46] as Type 1 shows that this estimate of f_e is consistent with data. We summarise the assumptions:

(i) Ion beam flux J_b is $n_b v_b$ with units of ions $\text{m}^{-2}\text{s}^{-1}$,
(ii) Ion beam is produced by diode mechanism [34],

(iii) The beam is produced uniformly across the whole cross-section of the pinch,
(iv) The beam speed is characterized by an average value v_b,
(v) The beam energy is a fraction f_e of the pinch inductive energy, taken as 0.14 in the first instance; to be adjusted as numerical experiments indicate,
(vi) The beam ion energy is derived from the diode voltage U,
(vii) The diode voltage U is $U=3V_{max}$; a relationship obtained from data fitting in extensive earlier numerical experiments [11, 14].

The value of the ion flux is deduced in each situation by computing Z_{eff}, r_p, I_{pinch} and U.

3. Numerical Experiments and Results

The Lee code is configured to work as any plasma focus by inputting the bank parameters, L_0, C_0 and stray circuit resistance r_0; the tube parameters b, a and z_0 and operational parameters V_0 and P_0 and the fill gas. The computed total current waveform is fitted to an experimentally measured total current waveform [11, 13-15, 28-29] using the four model parameters f_m, f_c for the axial phase and f_{mr} and f_{cr} for the radial phases.

3.1 Scaling laws for neutrons from numerical experiments over a range of energies from 10kJ to 25 MJ

We apply the Lee model code to the MJ machine PF1000 over a range of C_0 to study the neutrons emitted by PF1000-like bank energies from 10kJ to 25 MJ.

First, we fitted a measured current trace to obtain the model parameters. A measured current trace of the PF1000 with C_0=1332 μF, operated at 27 kV, 3.5 torr deuterium, has been published [34], with cathode/anode radii b=16 cm, a=11.55 cm and anode length z_0=60 cm. In the numerical experiments we fitted external (or static) inductance L_0= 33.5 nH and stray resistance r_0 = 6.1 mΩ (damping factor $RESF= r_0/(L_0/C_0)^{0.5}$ = 1.22). The fitted model parameters are: f_m=0.13, f_c=0.7, f_{mr}=0.35 and f_{cr}=0.65. The computed current trace [11, 15] agrees very well with the measured trace through all the phases; axial and radial, right down to the bottom of the current dip indicating the end of the pinch phase as shown in figure 1.

This agreement confirms the model parameters for PF1000. Once the model parameters have been fitted to a machine for a given gas, these model parameters may be used with some degree of confidence when operating parameters such as the voltage are varied [9].

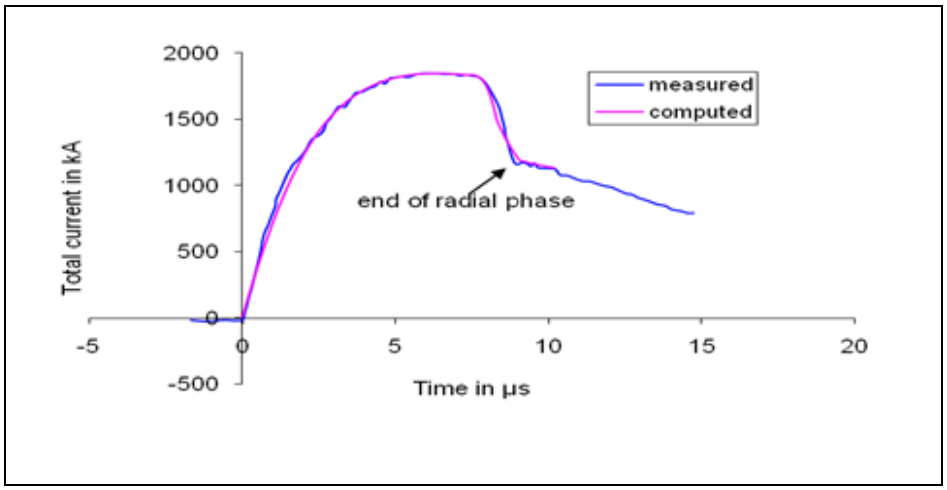

Figure 1. Current fitting of computed current to measured current traces to obtain fitted parameters f_m= 0.13, f_c= 0.7, f_{mr} = 0.35 and f_{cr}= 0.65.

This series is carried out at 35 kV, 10 Torr D, L_0=33.5 nH, r_0=6.1 mΩ (damping factor $RESF=r_0/(L_0/C_0)^{0.5}$ =1.22). The ratio $c=b/a$ is kept at 1.39; C_0 ranges from 14 μF to 39960 μF corresponding E_0 of 8.5 kJ to 24 MJ [12]. For each C_0, anode length z_0 is varied to find the optimum. For each z_0, a is varied so that end axial speed is 10 cm/μs.

We find that the Y_n scaling changes from $Y_n \sim E_0^{2.0}$ at tens of kJ to $Y_n \sim E_0^{0.84}$ at the highest energies (up to 25MJ) investigated (figure 2).

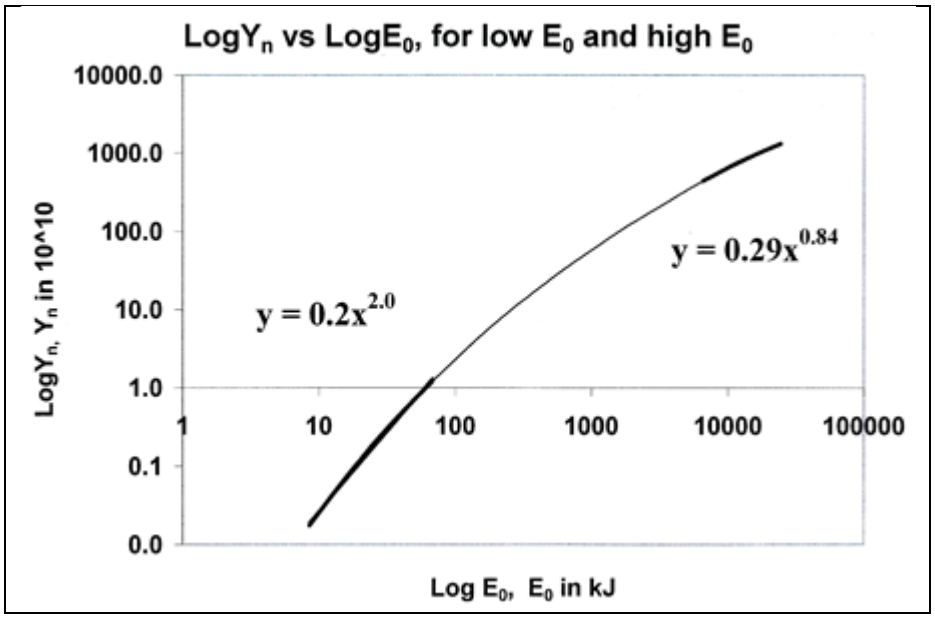

Figure 2. Y_n plotted as a function of E_0 in log-log scale, showing Y_n scaling changes from $Y_n \sim E_0^{2.0}$ at tens of kJ to $Y_n \sim E_0^{0.84}$ at the highest energies (up to 25MJ). The scaling deterioration observed in this figure is discussed in the Conclusion section.

The scaling of Y_n with I_{peak} and I_{pinch} over the energy range up to 25 MJ (figure 3) is: $Y_n = 3.2\times10^{11} I_{pinch}^{4.5}$ and $Y_n = 1.8\times10^{10} I_{peak}^{3.8}$ where I_{peak} ranges from 0.3 to 5.7 MA and I_{pinch} ranges from 0.2 to 2.4 MA.

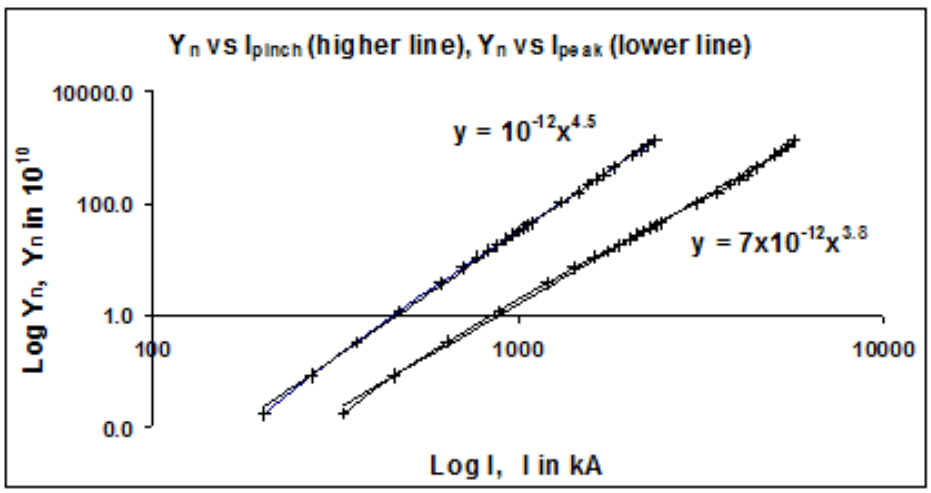

Figure 3. Log(Y_n) scaling with log(I_{peak}) and log(I_{pinch}) for the range of energies up to 25 MJ.

This scaling result confirms an earlier study carried out on several machines with published current traces with Y_n yield measurements, operating conditions and machine parameters including the PF400, UNU/ICTP PFF, the NX2 and Poseidon [11].

4. Scaling laws for neon SXR from numerical experiments over a range of energies from 0.2 kJ to 1 MJ

We next use the code to carry out numerical experiments for bank energies from 0.2 kJ to 1 MJ [52] using a fast PF machine with optimised values for c and typical low L_0.

The following parameters are kept constant: (i) $c=b/a$ (kept at 1.5, which is practically optimum; (ii) the operating voltage V_0 (kept at 20 kV); (iii) static inductance L_0 (kept at 30 nH, which is low enough to reach the I_{pinch} limitation regime [13,14] and (iv) ratio of stray resistance to surge impedance *RESF* (kept at 0.1). The model parameters [8-14] f_m, f_c, f_{mr}, f_{cr} are also kept at fixed values 0.06, 0.7, 0.16 and 0.7 representing average values of large range of machines we have studied. A typical current waveform is shown in figure 4.

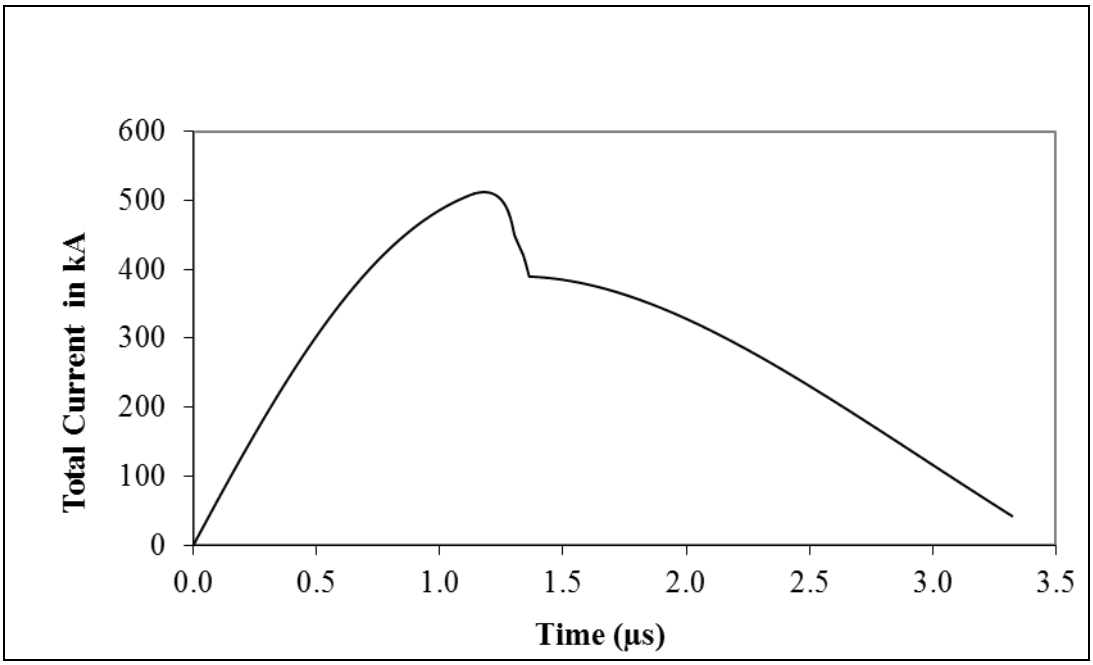

Figure 4. Computed total current versus time for L_0=30nH and V_0=20kV, C_0=30uF, *RESF*=0.1, c=1.5 and model parameters f_m, f_c, f_{mr}, f_{cr} are fixed at 0.06, 0.7, 0.16 and 0.7 for optimised a=2.285 cm and z_0=5.2 cm.

The storage energy E_0 is varied by changing the capacitance C_0. Parameters that are varied are operating pressure P_0, anode length z_0 and anode radius a. Parametric variation at each E_0 follows the order; P_0, z_0 and a until all realistic combinations of P_0, z_0 and a are investigated; the number of runs totalling some 2000. A plot of Y_{sxr} against E_0 is shown in figure 5.

We then plot Y_{sxr} against I_{peak} and I_{pinch} and obtain SXR yield scales as Y_{sxr}~$I_{pinch}^{3.6}$ and Y_{sxr}~$I_{peak}^{3.2}$. The I_{pinch} scaling has less scatter than the I_{peak} scaling. We next subject the scaling to further test when the fixed parameters *RESF*, c, L_0 and V_0 and model parameters f_m, f_c, f_{mr}, f_{cr} are varied. We add in the results of some numerical experiments using the parameters of several existing plasma focus devices including the UNU/ICTP PFF [17, 26] (*RESF*=0.2, c=3.4, L_0=110nH and V_0=14kV with fitted model parameters f_m = 0.05, f_c = 0.7, f_{mr} = 0.2, f_{cr} = 0.8) [7-9, 23], the NX [10, 24, 27] (*RESF* = 0.1, c = 2.2, L_0 = 20nH and V_0 =11 kV with fitted model parameters f_m = 0.06, f_c = 0.7, f_{mr} = 0.16, f_{cr} = 0.7) [7-10, 24] and PF1000 (*RESF*=0.1, c=1.39, L_0=33nH and V_0=27kV with fitted model parameters f_m=0.1, f_c=0.7,

f_{mr}=0.15, f_{cr}=0.7) [7-9,14]. These new data points (un-blackened data points in figure 6) contain wide ranges of c, V_0, L_0 and model parameters. The resulting Y_{sxr} versus I_{pinch} log-log curve remains a straight line, with scaling index 3.6 unchanged and with no increased scatter. However the resulting Y_{sxr} versus I_{peak} curve now exhibits larger scatter and the scaling index has changed.

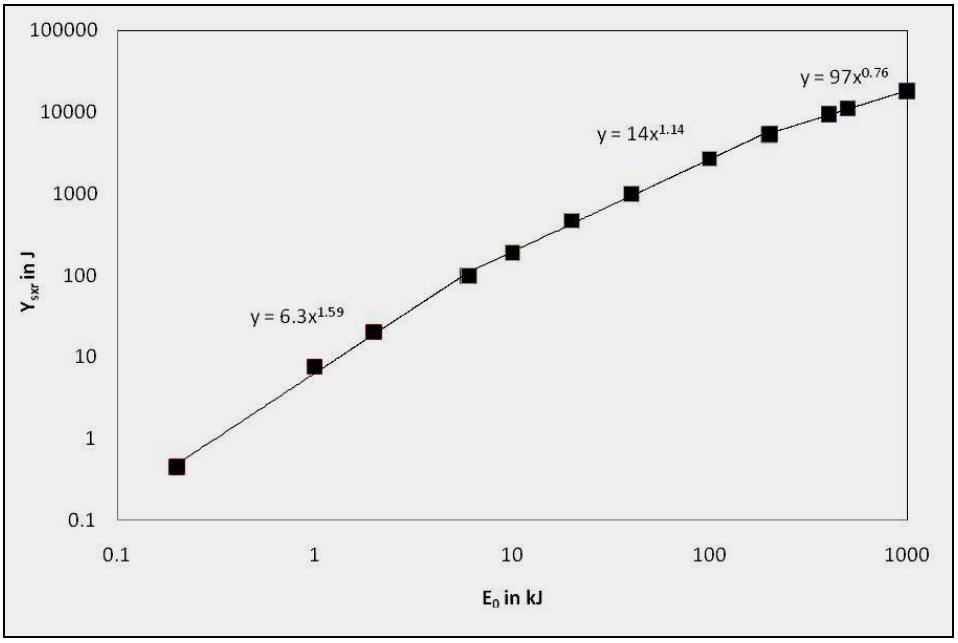

Figure 5. Y_{sxr} vs E_0. The parameters kept constants are: *RESF*=0.1, c=1.5, L_0=30nH and V_0=20 kV and model parameters f_m, f_c, f_{mr}, f_{cr} at 0.06, 0.7, 0.16 and 0.7 respectively. The scaling deterioration observed in this figure is discussed in the Conclusion section.

We highlight that the consistent behaviour of I_{pinch} in maintaining the scaling of $Y_{sxr} \sim I_{pinch}^{3.6}$ with less scatter than the $Y_{sxr} \sim I_{peak}^{3.2}$ scaling particularly when mixed-parameters cases are included, strongly support the conclusion that I_{pinch} scaling is the more universal and robust one. Similarly conclusions on the importance of I_{pinch} in plasma focus performance and scaling laws have been reported [11-15].

It is remarkable that our I_{pinch} scaling index of 3.6, obtained through a set of comprehensive numerical experiments over a range of energies 0.2 kJ to 1 MJ, on Mather-type devices is within the range of 3.5 to 4 postulated on the basis of sparse experimental data, (basically just two machines one at 5 kJ and the other at 0.9 MJ), by Filippov [6], for Filippov configurations in the range of energies 5 kJ to 1 MJ.

We point out that the results represent scaling for comparison with baseline PF devices that have been optimized in terms of electrode dimensions. It must also be emphasized that the scaling with I_{pinch} works well even when there are variations in device from L_0 =30 nH, V_0 =20 kV and c=1.5. However there may be many other parameters which can change and could lead to a further enhancement of x-ray yield.

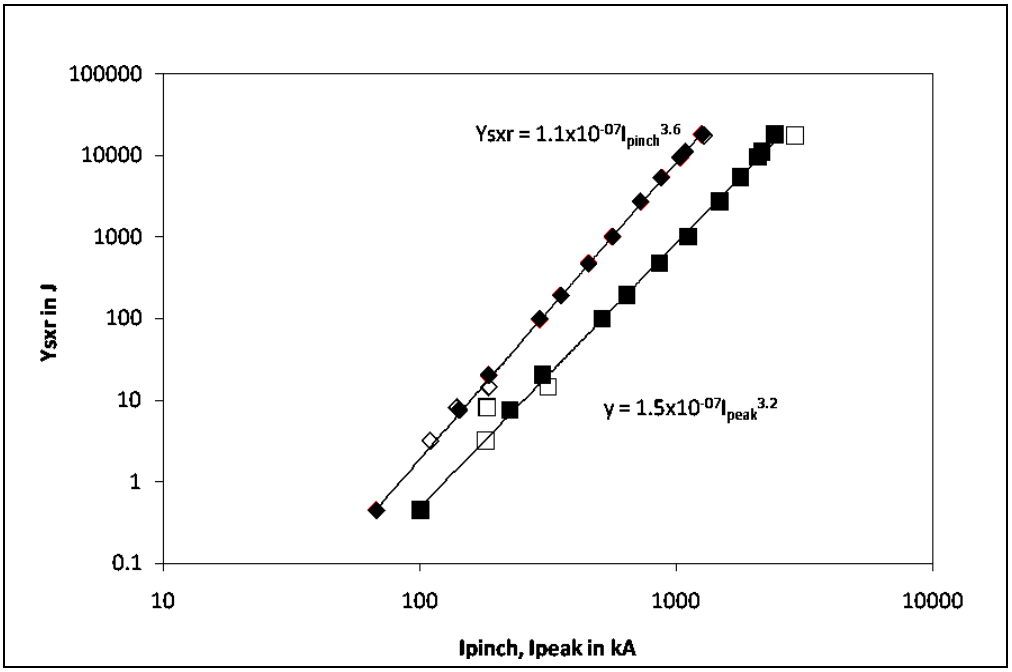

Figure 6. Y_{sxr} is plotted as a function of I_{pinch} and I_{peak}. The parameters kept constant for the black data points are: *RESF* = 0.1, c = 1.5, L_0 = 30nH and V_0 = 20 kV and model parameters f_m, f_c, f_{mr}, f_{cr} at 0.06, 0.7, 0.16 and 0.7 respectively. The unblackened data points are for specific machines which have different values for the parameters c, L_0, V_0 and *RESF*.

5. Scaling Laws for Beam Ions

Another set of series of numerical experiments on machines from sub-kJ to 1 MJ [50,51] were carried out to obtain relevant scaling laws for ions beam emitted from the pinch plasma. The results for PF deuteron beams (beam energy versus E_0) is presented in figure 7.

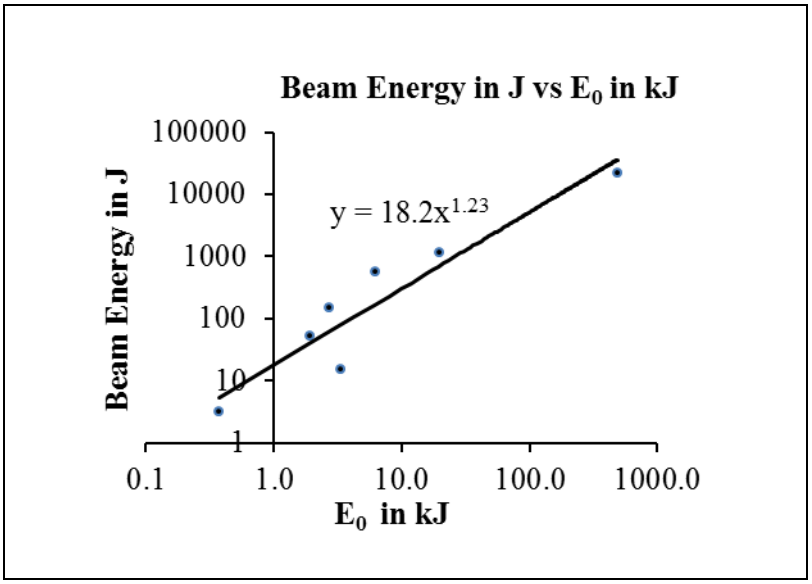

Figure 7. Establishing a first scaling law for deuteron beam energy in the plasma focus.

The beam ions (in J) at exit of a deuterium plasma pinch dependent of the currents (in kA) have the following scaling: $Y_{\text{beamions}}=2.8\text{x}10^{-7}I_{\text{pinch}}^{3.7}$; $Y_{\text{beamions}}=8.4\text{x}10^{-7}I_{\text{peak}}^{3.16}$; $Y_{\text{beamions}}=18.2E_0^{1.23}$; where Y_{beamions} is in J and E_0 is in kJ ranging from 1 kJ to 1MJ.

We note the considerable scatter with square of residual 'R^2' of 0.89, deviating considerably from the perfect value of 1.00 in this initial attempt to present quantitative ideas of ion beams to provide reference data for laboratory measurements. More numerical experiments and laboratory measurements are needed to put the scaling laws on a firmer footing.

The PF operating in any gas and over a wide range of pressure emits ion beams and plasma streams. These ion beams are being studied to synthesize nano-materials and damage candidate materials of reactor walls. The Lee model code computes the ion beam yields emitted from the pinch column.

6. Conclusion

Numerical experiments carried out using the universal plasma focus laboratory facility based on the Lee model code gives reliable scaling laws for neutrons production and neon SXR yields for plasma focus machines. The scaling laws obtained:

For neutron yield: (yield in number of neutrons per shot)
$Y_{\text{n}} = 3.2\text{x}10^{11} I_{\text{pinch}}^{4.5}$; $Y_n = 1.8\text{x}10^{10} I_{\text{peak}}^{3.8}$; I_{peak}(0.3 to 5.7) and I_{pinch}(0.2 to 2.4) in MA.
$Y_{\text{n}}\sim E_0^{2.0}$ at tens of kJ to $Y_{\text{n}}\sim E_0^{0.84}$ at MJ level (up to 25MJ).

For neon soft x-rays: (yield in J per shot)
$Y_{\text{sxr}} = 8.3\text{x}10^{3} I_{\text{pinch}}^{3.6;}$ $Y_{\text{sxr}} = 6\text{x}10^{2} I_{\text{peak}}^{3.2}$; I_{peak}(0.1 to 2.4) and I_{pinch}(0.07 to1.3) in MA.
$Y_{\text{sxr}}\sim E_0^{1.6}$ (kJ range) to $Y_{\text{sxr}}\sim E_0^{0.8}$ (towards MJ).

For beam ions at exit of a deuterium plasma pinch: (yield in J per shot)
$Y_{\text{beamions}}=2.8\text{x}10^{-7}I_{\text{pinch}}^{3.7}$; $Y_{\text{beamions}}= 8.4\text{x}10^{-7}I_{\text{peak}}^{3.16}$; and currents in kA.
$Y_{\text{beamions}}= 18.2E_0^{1.23}$; where E_0 is in kJ; averaged over 1 kJ to 1MJ

These laws provide useful references and facilitate the understanding of present plasma focus machines. More importantly, these scaling laws are also useful for design considerations of new plasma focus machines particularly if they are intended to operate as optimized neutron or neon SXR sources. More recently, the scaling of Y_{n} versus E_0 as shown above has been placed in the context of a global scaling law [38] with the inclusion of available experimental data. From that analysis, the cause of scaling deterioration for neutron yield versus energy as shown in figure 2 (which has also been given the misnomer 'neutron saturation') has been uncovered as due to a current scaling deterioration caused by an almost constant axial phase 'dynamic resistance' interacting with a reducing bank impedance as energy storage is increased at essentially constant voltage. The deterioration of soft x-ray yield with storage energy as shown in figure 5 could also be ascribed to the same axial phase 'dynamic resistance' effect as described in reference [38]. This deterioration of scaling will also appear in the scaling trends (with stored energy) of beam ions.

We emphasis here that the scaling laws with I_{pinch} is the more fundamental and robust one compared to I_{peak}. This is because although the PF is reasonably consistent in its operations, there will be occasions when even the best optimized machines may not focus or poorly focused although having a high I_{peak} with no neutrons. However, I_{pinch} being the current actually flowing in the pinch is more consistent in all situations.

The numerical experiments gives robust scaling laws for PFs covering a wide range of energies from sub kJ to tens of MJ. It supplements the limited (non-existent in the case of beam ions) scaling laws available to predict PF radiations yields. Now, we have on stronger footing the useful scaling laws for neutron, SXR and ion yields from PF machines.

7. References

[1] Lee S 1998 *Twelve years of UNU/ICTP PFF—A Review* IC/ 98/ 231 Abdus Salam ICTP, Miramare, Trieste ICTP Open Access Archive http://eprints.ictp.it/31/ 5-34
[2] Kato Y and Be S H 1986 *Appl. Phys. Lett.* **48** 686
[3] Bogolyubov E P et al 1998 *Phys. Scripta*. **57** 488-494
[4] Lee S et al 1998 *IEEE Trans. Plasma Sci.* **26** 1119
[5] Filippov N V et al 1996 *IEEE Trans Plasma Sci.* ***24*** 1215-1223
[6] Filippov N V et al 1996 *Phys Lett A* **211**(3) 168-171
[7] Lee S *Institute for Plasma Focus Studies* http://www.plasmafocus.net
[8] Lee S *Internet Workshop on Plasma Focus Numerical Experiments(IPFS-IBC1)14April-19May 2008* http://www.plasmafocus.net/IPFS/Papers/IWPCAkeynote2ResultsofInternet-basedWorkshop.doc
[9] Lee S *Radiative Dense Plasma Focus Computation Package: RADPF* http://www.intimal.edu.my/school/fas/UFLF/File1RADPF.htm http://www.plasmafocus.net/IPFS/modelpackage/File1RADPF.htm
[10] Lee S, Rawat R S, Lee P and Saw S H 2009 *J. Appl. Phys*. **106** 023309
[11] Lee S and Saw S H 2008 *J Fusion Energy* **27** 292-295
[12] Lee S 2008 *Plasma Phys. Control. Fusion* **50** 105005
[13] Lee S, Saw S H, Lee P C K, Rawat R S and Schmidt H 2008 *Appl. Phys. Lett.* **92** 111501
[14] Lee S and Saw S H 2008 *Appl. Phys. Lett.* **92** 021503
[15] Lee S, Lee P, Saw S H and Rawat R S 2008 *Plasma Phys. Control. Fusion* **50** 065012
[16] Lee S, 1984 Plasma focus model yielding trajectory and structure in *Radiations in Plasmas*, ed B McNamara (Singapore: World Sci Pub Co, ISBN 9971-966-37-9) vol. II 978–987
[17] Lee S et al 1988 *Am. J. Phys*. **56** 62-68
[18] Tou T Y, Lee S and Kwek K H 1989 *IEEE Trans. Plasma Sci.* **17** 311-315
[19] Lee S 1991 *IEEE Trans. Plasma Sci*. **19** 912-919
[20] Jalil bin Ali 1990 *Development and Studies of a small Plasma Focus* PhD thesis, Universiti Teknologi Malaysia, Malaysia
[21] Potter D E 1978 *Nucl. Fus*. **18** 813-823
[22] Lee S and Serban A 1996 *IEEE Trans. Plasma Sci.* **24**(3) 1101-1105.
[23] Liu Mahe 2006 *Soft X-rays from compact plasma focus* PhD thesis, NIE, Nanyang Technological University, Singapore. ICTP Open Access Archive: http://eprints.ictp.it/327/
[24] Bing S 2000 *Plasma dynamics and x-ray emission of the plasma focus* PhD Thesis, NIE, Nanyang Technological University, Singapore. ICTP Open Access Archive: http://eprints.ictp.it/99/.
[25] Serban A and Lee S 1998 *J Plasma Physics* **60**(1) 3-15.
[26] Liu M H, Feng X P, Springham S V and Lee S 1998 *IEEE Trans. Plasma Sci.* **26** 135–140
[27] Wong D, Lee P, Zhang T, Patran A, Tan T L, Rawat R S and Lee S *2007 Plasma Sources Sci. Technol.* **16** 116-123
[28] Lee S 2000–2007 http://ckplee.myplace.nie.edu.sg/plasmaphysics/
[29] Lee S 2005 ICTP Open Access Archive: http://eprints.ictp.it/85/
[30] Mohammadi M A, Sobhanian S, Wong C S, Lee S, Lee P and Rawat R S 2009 *J. Phys. D: Appl.Phys.* **42** 045203
[31] Springham S V, Lee S and Rafique M S 2000 *Plasma Phys. Control. Fusion* **42** 1023-1032
[32] Lee S, Lee P, Zhang G, Feng X, Gribkov V A, Liu M, Serban A and Wong T 1998 *IEEE Trans. Plasma Sci.* **26**, no. 4 1119-1126
[33] Siahpoush V, Tafreshi M A, Sobhanian S and Khorram S 2005 *Plasma Phys. Control. Fusion* **47** 1065-1072
[34] Gribkov V A, Banaszak A, Bienkowska B, Dubrovsky A V, Ivanova-Stanik I, Jakubowski L, Karpinski L, Miklaszewski R A, Paduch M, Sadowski M J, M Scholz M, A Szydlowski and Tomaszewski K 2007 *J. Phys. D: Appl. Phys*. **40** 3592-3607.

[35] Lee S 2009 *Appl. Phys. Lett.* **95** 151503
[36] Lee S, Saw S H and Jalil Ali 2013 *J Fusion Energy* **32** 42-49
[37] Lee S and S H Saw 2012, *J Fusion Energy* **31** 603-610
[38] Saw S H 1991 *Experimental studies of a current-stepped pinch* PhD Thesis Universiti Malaya, Malaysia
[39] Lee S 1984 J *Phys D: Appl Phys* **17**,733-739
[40] Lee S et al 2011 *IEEE Trans Plasma Sci* **39** 3196-3202
[41] Saw S H et al 2010 Rev Sci Instruments, **81** 053505
[42] Lee S et al 2012 *J Fusion Energy* **31** 198–204
[43] Lee S, Saw S H, Soto L, Springham S V, Moo S P 2009 *Plasma Phys Contr Fusion* **51** 075006
[44] Saw S H, Rawat R S, Lee P, Talebitaher Alireza, Abdou A E, Chong P L, Roy F Jr, Ali J and Lee S 2013 *IEEE Trans Plasma Sci* **41** (11) 3166-3172
[45] Lee S, Saw S H, Hegazy H, Ali J, Damideh V, Fatis N, Kariri H, Khubrani A, Mahasi A *J Fusion Energy* published online 5 January 2014
[46] Lee S, Saw S H, Abdou A E and Torreblanca H 2011 *J Fusion Energy* **30**, 277-282
[47] Aghamir F M and Behbahani R A 2012 *J. Plasma Physics* **78**(5) 585-588
[48] M. Akel, Sh Al-Hawat, S H Saw and S Lee 2010 *J Fusion Energy* **29(**3) 223-231
[49] Sh. Al-Hawat, M. Akel, S H Saw, S Lee 2012 J Fusion Energy **31** 13-20
[50] Akel M, Lee S, Saw S H, *IEEE Trans Plasma Sci* **40** 3290-3297
[51] Huba J D 2006 *Plasma Formulary* 44
[52] Lee S, Saw S H, Lee P and Rawat R S 2009 *Plasma Phys and Controlled Fusion* **51** 105013
[53] Lee S and Saw S H 2012 *Phys. Plasmas* **19** 112703
[54] Lee S and Saw S H 2013 *Phys. Plasmas* **20** 062702

Acknowledgments
This work is partially supported within IAEA Research Contract: 16934 of CRP F1.30.13 (Investigations of Materials under High Repetition and Intense Fusion-relevant Pulses). The author also acknowledges research grants INT-CPR-01-02-2012 and FRGS/2/2013/SG02/INTI/01/1.